

RESEARCH ARTICLE

Antimicrobial peptide activity is anticorrelated with lipid a leaflet affinity

Nathaniel Nelson¹, Belita Opene², Robert K. Ernst², Daniel K. Schwartz^{1*}

1 Department of Chemical and Biological Engineering, University of Colorado Boulder, Boulder, Colorado, United States of America, **2** Department of Microbial Pathogenesis, School of Dentistry, University of Maryland Baltimore, Baltimore, Maryland, United States of America

* daniel.schwartz@colorado.edu

Abstract

The activity of antimicrobial peptides (AMPs) has significant bacterial species bias, the mechanisms of which are not fully understood. We employed single-molecule tracking to measure the affinity of three different AMPs to hybrid supported bilayers composed of lipid A extracted from four different Gram negative bacteria and observed a strong empirical anticorrelation between the affinity of a particular AMP to a given lipid A layer and the activity of that AMP towards the bacterium from which that lipid A was extracted. This suggested that the species bias of AMP activity is directly related to AMP interactions with bacterial outer membranes, despite the fact that the mechanism of antimicrobial activity occurs at the inner membrane. The trend also suggested that the interactions between AMPs and the outer membrane lipid A (even in the absence of other components, such as lipopolysaccharides) capture effects that are relevant to the minimum inhibitory concentration.

OPEN ACCESS

Citation: Nelson N, Opene B, Ernst RK, Schwartz DK (2020) Antimicrobial peptide activity is anticorrelated with lipid a leaflet affinity. PLoS ONE 15(11): e0242907. <https://doi.org/10.1371/journal.pone.0242907>

Editor: Surajit Bhattacharjya, Nanyang Technological University, SINGAPORE

Received: September 23, 2020

Accepted: November 12, 2020

Published: November 30, 2020

Copyright: © 2020 Nelson et al. This is an open access article distributed under the terms of the [Creative Commons Attribution License](https://creativecommons.org/licenses/by/4.0/), which permits unrestricted use, distribution, and reproduction in any medium, provided the original author and source are credited.

Data Availability Statement: All relevant data are within the paper and its [Supporting Information](#) files.

Funding: NN and DKS acknowledge support from the U.S. Army Research Office under grant number W911NF-16-1-0151. RKE acknowledges support from the NIH (R01AI147314).

Competing interests: The authors have declared that no competing interests exist.

Introduction

The activity of antimicrobial peptides (AMPs) towards different Gram-negative bacteria, while not truly specific, is highly variable in ways that are not easily predictable. The variability of AMPs appears counter-intuitive at first glance, since the mechanism of AMP activity is associated with the degradation, through pores [1] or carpet assembly [2] of the *inner* bacterial membrane, which is composed of a highly conserved phospholipid bilayer. This suggests that the species-bias of AMPs may instead be traced to the outer bacterial membrane [3], which is the first barrier encountered by AMPs, and must be translocated to reach the inner membrane. The outer membrane is asymmetric, with an outer leaflet comprising primarily lipid A (and lipid-A-containing lipopolysaccharides) and a phospholipid inner leaflet [4]. Lipid A exhibits enormous structural variability, in fact lipid A structure and composition can serve as a signature of bacterial identity [5].

The mechanism of AMP activity towards bacteria is complex, comprising binding, translocation, self-assembly, and other processes. It is well established that strong binding to bacterial surfaces is necessary for AMP activity. Measurements of AMP binding to whole bacteria have shown that AMPs show affinity towards bacterial strains upon which they exhibit antimicrobial activity, and also that activity is associated with high AMP surface coverage [6,7].

Biophysical methods, such as NMR and isothermal titration calorimetry have demonstrated that AMPs bind strongly to outer membrane components (e.g. in the form of lipopolysaccharide micelles), and that this binding influences AMP secondary structure [8–11]. Here, we employ a model system to isolate and explore one part of this complex process, the strength of interactions between individual AMP molecules and lipid A. The interest in this particular process was motivated by the fact that biosynthetic modifications of lipid A are often observed to be associated with AMP resistance [12]. Thus, it is plausible to hypothesize that distinctive physico-chemical AMP/lipid A interactions may be related the variable activity of particular AMPs towards different bacteria.

The structure of lipid A comprises 4–7 aliphatic tails (of varying length and saturation), a disaccharide head group, and 0–2 negatively charged phosphate groups [13,14], leading to an enormous number of possible variations. Since most AMPs are positively charged, electrostatic attraction is apparently an important component of AMP/lipid A interactions [15,16]. Hydrophobic interactions have also been shown to influence interactions between AMPs and lipid A. Considering that a given outer bacterial membrane may contain a heterogeneous mixture of lipid A species as well as other lipopolysaccharide components, AMP-lipid A affinity is difficult to predict. Moreover, using traditional methods, it has been challenging to measure isolated AMP interactions with lipid A leaflets in a bilayer geometry. We employed a single-molecule fluorescence imaging method that was capable of quantitatively measuring the affinity between AMPs and hybrid lipid bilayers with a lipid A outer leaflet under steady state conditions, thereby isolating the effects of AMP-lipid A interactions in a relevant geometry.

We previously developed an approach to characterize relevant AMP–lipid A interactions using single-molecule super-resolution imaging to track fluorescently labeled AMPs as they interacted with asymmetric supported lipid bilayer (SLBs) outer membrane mimics [17]. By measuring AMP coverage, adsorption/desorption dynamics, and interfacial diffusion, we showed that this approach was sensitive to subtly different interactions between AMPs and lipid A asymmetric bilayers composed of diphosphoryl and hexa-acylated, monophosphoryl *E. coli* lipid A. Here, we employed this approach to characterize the interactions between three different AMPs, and asymmetric bilayers comprising complex lipid A mixtures isolated from four different Gram-negative bacteria: *Acinetobacter baumannii* (AB), *Klebsiella pneumoniae* (KP), *Pseudomonas aeruginosa* (PA), and *Escherichia coli* (EC), and found a distinctive empirical relationship between the strength of these physical interactions and to the activity of AMPs towards the bacterial species from which the lipid A were extracted.

Materials and methods

The AMPs used in this work—LL37 (LL), Cecropin B (CEC), and Melittin (MEL)—exhibit an amphipathic α -helical structure when interacting with a lipid bilayer but are unstructured in solution [18,19] and have nominal charges of +5, +7, and +6, respectively under physiological conditions. LL37 is a human peptide sequence, Cecropin B is isolated from a giant silk moth, and Melittin is found in bee venom. All three have antimicrobial activity against Gram-negative bacteria; CEC and MEL also show activity against other microbes and tumor cells. We characterized the interactions of these AMPs with asymmetric SLBs incorporating reconstituted lipid A extracted from all four bacterial backgrounds. Structural information about the AMPs is summarized in Table 1.

As described previously [17], we employed a Langmuir-Blodgett/Langmuir-Schaefer (LB/LS) layer-by-layer deposition approach to create asymmetric SLBs with an exposed outer leaflet comprising lipid A and a 1,2-dioleoyl-sn-glycero-3-phosphoethanolamine (DOPE) inner leaflet. In the present study, the lipid A in a given experiment was reconstituted from material

Table 1. Structures of antimicrobial peptides.

Peptide	Primary Sequence	Secondary Structure
LL-37	LLGDFFRKSKEKIGKEFKRIVQRIKDFLRNLPRTES	primarily helical [20]
Cecropin B	KWKVFKKIEKMGRNIRNGIVKAGPAIAVLGEAKAL	helix-hinge-helix [21,22]
Melittin	GIGAVLKVLTTGLPALISWIKRKRQQ	primarily helical [23]

<https://doi.org/10.1371/journal.pone.0242907.t001>

isolated from the organism of interest [24]. Large-scale bacterial LPS preparations were isolated using a hot phenol/water extraction method after growth in lysogenic broth supplemented with 1mM MgCl₂ at 37 °C [25]. Subsequently, LPS was treated with RNase A, DNase I and proteinase K to ensure purity from contaminating nucleic acids and proteins [26]. Individual LPS samples were additionally extracted to remove contaminating phospholipids [27] and TLR2 contaminating proteins [28]. Finally, individual LPS preparations were resuspended in 500 ml of water, frozen on dry ice and lyophilized. Lipid A was isolated after hydrolysis in 1% SDS at pH 4.5 as described previously [29].

Lipid bilayers were formed using a LB/LS deposition technique using a NIMA Langmuir trough (KSV NIMA, Espoo, Finland). Lipid A samples were dissolved at a concentration of 1 mg/mL in a 73:24:3 (v:v) mixture of chloroform:methanol:water. DOPE (Avanti Polar Lipids, Alabaster, AL) was dissolved in chloroform at a concentration of 1 mg/mL. Lipids were deposited to the air/water interface by adding 20 mL of lipid A solution or 30 mL of DOPE solution in 2 mL increments. The lipids were then compressed to a surface pressure of 27 mN/m and maintained at 21 ± 0.5 °C. Pieces of 25x25 mm #1 cover glass (ThermoFisher Scientific) were cleaned with hot piranha solution (30% hydrogen peroxide/70% sulfuric acid by volume) at 50 °C for 1 h, followed by thorough rinsing in Milli-Q water (Millipore) and drying under ultrapure nitrogen. The dry coverslips were then placed in an ultraviolet (UV)-ozone chamber (PSD series Digital UV Ozone System; Novascan, Ames, IA) for 1 h and used within 20 min of removal from the UV-ozone chamber.

To deposit the inner SLB leaflet, a clean coverslip was first submerged into the Langmuir trough; DOPE was then deposited at the air/water interface. The coverslip, oriented vertical to the interface, was drawn through the lipid monolayer at the air-water interface at a rate of 3 mm/min, depositing a phospholipid monolayer with the head group toward the glass substrate. During monolayer deposition, the surface pressure was held at a constant 27 mN/m through a feedback loop, which yielded monolayers with estimated areas per molecule of 0.55 nm² for DOPE and 1.2 nm² for lipid A. Previous work has shown these to be representative molecular areas for lipids in biological membranes, and appropriate models to study interactions between AMP and lipid A at the air-water interface [30,31]. After inner leaflet deposition, the remaining lipid monolayer at the air-water interface of the Langmuir trough was removed through pipette aspiration. Outer leaflet lipid A was then deposited and compressed using the Langmuir trough. The substrate with deposited inner leaflet was then rotated parallel to the plane of the air/water interface and lowered onto the freshly formed monolayer forming an SLB and passing into the aqueous phase. The resulting SLB was kept submerged in 1x PBS to avoid bilayer disruption.

Peptides were synthesized by GenScript (Piscataway, NJ) with an unnatural azido-lysine amino acid at the C-terminus, enabling fluorescent labeling via copper-free strained alkyne click reaction chemistry [32]. Peptides were dissolved in 1x PBS at room temperature at a concentration of 2 mg/mL. Alexa Fluor 488 dibenzocyclooctyne alkyne (ThermoFisher Scientific, Waltham, MA) was dissolved in dimethyl sulfoxide at a concentration of 2.5 mg/mL. The peptide and fluorophore solutions were mixed at a 3:2 molar ratio of peptide to fluorophore and reacted for 24 h at 4 °C. The resultant solution was then passed through a reversed-phase

chromatography column (SEC 70 10 x 300 mm column; Bio-Rad, Hercules, CA) at 1 mL/min using PBS and the fluorescent fraction was isolated.

Super-resolution single-molecule total internal reflection fluorescence microscopy was employed to localize and track individual fluorescently labeled AMP molecules as they adsorbed to, diffused on, and desorbed from the bilayer surface. Time series of images, with 100ms acquisition time, were captured on an inverted Nikon Eclipse Ti Microscope with a Plan-Apo 100x 1.45 NA oil immersion objective (Nikon, Melville, NY) using a Hamamatsu CMOS camera. Excitation light generated by a 100 mW 491 nm solid-state laser (Cobolt Calypso 100; Cobolt) was passed through a total internal reflection illuminator (TI-TIRF-EM; Nikon) to generate an evanescent field at the SLB-water interface with incident energy of $\sim 0.75 \text{ kW/cm}^2$. All microscopy experiments were performed at $21 \pm 0.5 \text{ }^\circ\text{C}$. At least three replicate experiments were performed for each experimental condition. Each experiment comprised at least five movies, with durations of approximately 10s, from independent fields of view. Single-molecule tracking was performed using a custom *Mathematica* script to identify and localize diffraction-limited spots [33,34]. At least 2,000 molecular trajectories were obtained for each experimental condition. The number of molecules was determined in each frame and used to calculate the average surface coverage. The standard error from replicate experiments was used to determine the uncertainty in the average surface coverage.

We focused on observations of the steady-state (equilibrium) surface density of AMPs (i.e., the adsorbed AMP mass per unit bilayer area) as it related to the concentration of AMP in solution. To measure the affinity of AMPs to lipid A leaflets at the low-concentration/low-surface density limit, AMPs were added to PBS (pH 7.4) buffer in contact with SLBs at a concentration of 10^{-10} M (which allowed for single-molecule localization) and allowed to equilibrate. Image sequences were then acquired in multiple locations, where the duration of the movies was short compared to the characteristic time constant for bleaching as in previous work. Adsorbed AMPs were localized and counted to determine the average equilibrium number of molecules adsorbed per surface area and converted to mass per area using the AMP molecular mass. The affinity was then calculated as the ratio of the AMP surface density to solution concentration:

$$\text{Affinity} = \frac{\text{AMP surface density (mg/m}^2\text{)}}{\text{solution concentration (mM)}}$$

Given the extremely low surface density (individual AMP molecules were typically separated by μm distances), and the fact that no significant differences in fluorescence intensity were observed between localized objects, AMP were presumed to be monomeric, which is an advantage of this SM approach in measuring surface affinity.

Results and discussion

[Fig 1](#) illustrates the main result of this article, plotting the measured AMP affinity vs. minimum inhibitory concentrations (MIC) associated with the antimicrobial activity of the same AMPs against the organisms from which the lipid A was extracted, for nine different AMP/lipid A combinations. The MIC values were drawn from a literature review, summarized in [Table 1](#), and reflect the variability of published MIC measurements. Each average MIC is indicated by a symbol, and the range of MIC values is spanned by the connected bars. With the exception of Melittin interaction with lipid A isolated from *A. baumannii*, the affinity exhibits a systematic anti-correlation with measured MIC values over more than one order of magnitude in both quantities. This empirical trend is consistent with the conjecture that the species bias of AMP activity is related to AMP interactions with bacterial outer membranes, despite the fact that the

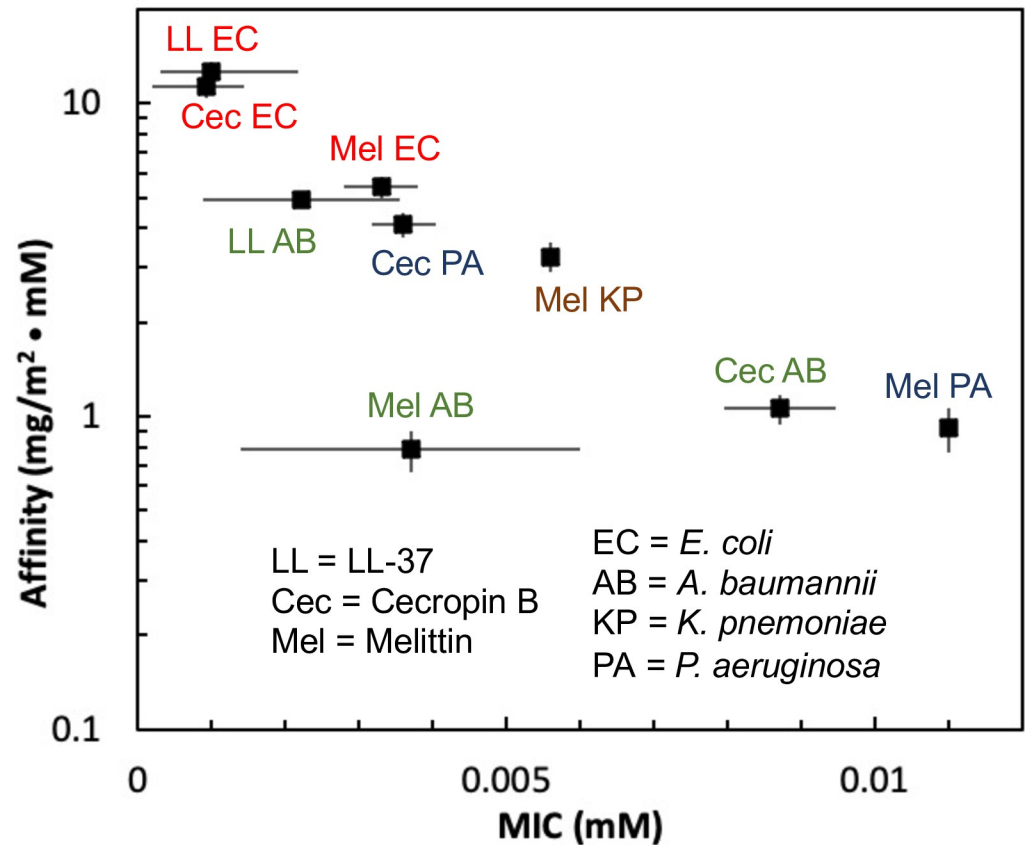


Fig 1. Semi-logarithmic plot of AMP affinity from single-molecule observations of fluorescent AMPs adsorbed on asymmetric hybrid bilayers composed of lipid A isolated from gram-negative bacteria. The data are plotted vs. the average of previously published MIC values. Table 2 summarizes the sources of the MIC values. The horizontal bars represent the full range of published values. The vertical bars represent the uncertainty in the mean affinity from replicate experiments as described in the main text. The numerical values of these data are tabulated in S1 Table in the Supporting Information.

<https://doi.org/10.1371/journal.pone.0242907.g001>

mechanism of antimicrobial activity occurs at the inner membrane. Moreover, while the outer membrane exhibits a complex structure, the trend also suggests that the interactions between AMPs and the outer membrane lipid A (even in the absence of other components, such as the carbohydrate portion of lipopolysaccharides) captures interactions that are relevant to the

Table 2. Sources of minimum inhibitory concentration values used in Fig 1.

Bacterium	Peptide	Sources of MIC values
<i>Acinetobacter baumannii</i>	Melittin	4 mg/L [35], 17 mg/L [36]
	LL-37	16 mg/L [37], 4 mg/L [38]
	Cecropin B	32 mg/L [35], 7.04 μM [39]
<i>Escherichia coli</i>	Melittin	8 mg/L [40], 3.8 μM [41]
	LL-37	2.1 mg/L [42], 9.8 mg/L [43], 0.312 μM [44]
	Cecropin B	0.2 μM [45], 1.17 μM [46], 1.43 μM [39]
<i>Pseudomonas aeruginosa</i>	Melittin	32 mg/L [40]
	Cecropin B	4 μM [45], 3.13 μM [46]
<i>Klebsiella pneumoniae</i>	Melittin	16 mg/L [40]

<https://doi.org/10.1371/journal.pone.0242907.t002>

minimum inhibitory concentration. This behavior is expected to be related to differences in lipid A structure among species and to complex interactions that are related to charge, hydrophobicity, membrane heterogeneity, and other factors.

It is possible that the fluorescent probe may have a modest influence on the interactions between the labeled peptide and lipid A; indeed this is a fundamental limitation of all fluorescence methods. However, since the same fluorescent label and conjugation method has been used in all cases, and the molecular weight of the label is small compared to that of the AMPs, it is plausible to infer that while the absolute affinities may be slightly perturbed due to the labeling, the general trends of affinity should still be representative of those associated with unlabeled AMPs.

SM-tracking experiments were also performed at higher solution AMP concentrations, similar to the MIC for each AMP-lipid A combination. In these experiments, the fluorescently labeled AMP concentration was maintained at the same low level to enable SM localization, and large amounts of unlabeled AMPs was added to bring the total concentration to the relevant values. The total surface density was then calculated by multiplying the apparent surface density of labeled AMP by the ratio of total AMP to labeled AMP. Even at higher concentrations corresponding to the MIC, the total surface coverage was found to be in the low coverage regime, where surface coverage is proportional to solution concentration. The values of surface coverage were in the range 0.003–0.018 mg/m², which represents less than 1% of a close-packed peptide monolayer.

In the context of classical Langmuir adsorption theory, the affinity is related to the equilibrium constant, $K \propto \exp(U_{ads}/k_B T)$, where U_{ads} is the potential energy of adsorption, k_B is Boltzmann's constant, and T is the absolute temperature. Thus, roughly speaking, $\ln K$ may be expected to provide information about the adsorption energy. The semi-logarithmic form of Fig 1 leads one to speculate that $\ln K \propto \text{MIC}$, which would be the case if the MIC were proportional to the adsorption energy of the AMP on the lipid A leaflet. While there is currently no existing theoretical basis to understand the connection of AMP adsorption to bacterial activity, this empirical relationship may form the basis of a plausible hypothesis for future testing and to guide theory.

Conclusions

The results shown Fig 1 demonstrate an empirical relationship between a *physical* measure of intermolecular interactions and a quantity representing *biological* activity. In particular, they show that the interfacial affinity of a given AMP to a lipid bilayer with a lipid A outer leaflet is anticorrelated with the activity of that AMP towards the Gram negative bacterial species from which the lipid A was extracted. That is, AMPs that interact more strongly with the lipid A in the bacterial outer membrane require a smaller dose to impart an inhibitory effect, and vice versa.

These data, while shown concisely in a single figure, represent a comprehensive study incorporating experiments that include three different AMPs and lipid A from four different bacterial organisms. Moreover, the trend connecting the values of affinity and MIC spans a substantial range of more than one order of magnitude in both quantities. This previously unknown relationship provides support for the hypothesis that AMP species bias is directly related to outer membrane interactions, with lipid A in particular, despite the fact that the effects of AMPs are known to occur at the inner membrane.

Presumably, the affinity measured here can be physically related to molecular level interactions between AMP and species-specific lipid A molecules. These interactions may be complex, and not simply related to one particular type of force. For example, the affinity between

an AMP and a lipid A layer may involve a combination of electrostatic, hydrophobic, and other non-covalent effects, which can potentially be probed using computational methods such as atomistic molecular dynamics simulations. The results presented here may stimulate computational studies that can isolate these interactions.

Importantly, the interactions between AMP molecules and lipid A leaflets reported here clearly represent only one small piece of a complex and diverse process that involves many steps and multiple molecular components. Our hope is that the empirical relationship identified in this manuscript will complement other biophysical studies of AMPs that employ various methods to explore interactions with other cellular components and structures, ultimately leading to a more comprehensive understanding.

Supporting information

S1 Table. Tabulated data displayed in Fig 1 of the text.
(DOCX)

Author Contributions

Conceptualization: Nathaniel Nelson, Robert K. Ernst, Daniel K. Schwartz.

Formal analysis: Nathaniel Nelson.

Funding acquisition: Robert K. Ernst, Daniel K. Schwartz.

Investigation: Nathaniel Nelson, Belita Opene, Robert K. Ernst.

Methodology: Nathaniel Nelson, Belita Opene, Robert K. Ernst.

Project administration: Robert K. Ernst, Daniel K. Schwartz.

Supervision: Daniel K. Schwartz.

Writing – original draft: Robert K. Ernst, Daniel K. Schwartz.

Writing – review & editing: Robert K. Ernst, Daniel K. Schwartz.

References

1. Yang L, Harroun TA, Weiss TM, Ding L, Huang HW. Barrel-stave model or toroidal model? A case study on melittin pores. *Biophys J.* 2001; 81(3):1475–85. [https://doi.org/10.1016/S0006-3495\(01\)75802-X](https://doi.org/10.1016/S0006-3495(01)75802-X) WOS:000170600800024. PMID: 11509361
2. Ambroggio EE, Separovic F, Bowie JH, Fidelio GD, Bagatolli LA. Direct visualization of membrane leakage induced by the antibiotic peptides: Maculatin, citropin, and aurein. *Biophys J.* 2005; 89(3):1874–81. <https://doi.org/10.1529/biophysj.105.066589> WOS:000231502800043. PMID: 15994901
3. Hancock REW. Antibacterial peptides and the outer membranes of gram-negative bacilli. *J Med Microbiol.* 1997; 46(1):1–3. WOS:A1997WB70100001. <https://doi.org/10.1099/00222615-46-1-1> PMID: 9003734
4. Beveridge TJ. Structures of gram-negative cell walls and their derived membrane vesicles. *J Bacteriol.* 1999; 181(16):4725–33. <https://doi.org/10.1128/JB.181.16.4725-4733.1999> WOS:000082012100001. PMID: 10438737
5. Liang T, Leung LM, Opene B, Fondrie WE, Lee YI, Chandler CE, et al. Rapid Microbial Identification and Antibiotic Resistance Detection by Mass Spectrometric Analysis of Membrane Lipids. *Anal Chem.* 2019; 91(2):1286–94. <https://doi.org/10.1021/acs.analchem.8b02611> WOS:000456350000013. PMID: 30571097
6. Roversi D, Luca V, Aureli S, Park Y, Mangoni ML, Stella L. How Many Antimicrobial Peptide Molecules Kill a Bacterium? The Case of PMAP-23. *Acs Chem Biol.* 2014; 9(9):2003–7. <https://doi.org/10.1021/cb500426r> WOS:000342121200015. PMID: 25058470
7. Savini F, Loffredo MR, Troiano C, Bobone S, Malanovic N, Eichmann TO, et al. Binding of an antimicrobial peptide to bacterial cells: Interaction with different species, strains and cellular components. *Bba-*

- Biomembranes. 2020; 1862(8). ARTN 183291. <https://doi.org/10.1016/j.bbamem.2020.183291> WOS:000537573200018. PMID: 32234322
8. Bhunia A, Domadia PN, Bhattacharjya S. Structural and thermodynamic analyses of the interaction between melittin and lipopolysaccharide. *Bba-Biomembranes*. 2007; 1768(12):3282–91. <https://doi.org/10.1016/j.bbamem.2007.07.017> WOS:000252488900033. PMID: 17854761
 9. Bhunia A, Domadia PN, Torres J, Hallock KJ, Ramamoorthy A, Bhattacharjya S. NMR Structure of Pore-forming Antimicrobial Peptide, in Lipopolysaccharide Micelles MECHANISM OF OUTER MEMBRANE PERMEABILIZATION. *J Biol Chem*. 2010; 285(6):3883–95. <https://doi.org/10.1074/jbc.M109.065672> WOS:000275254000042. PMID: 19959835
 10. Bhunia A, Saravanan R, Mohanram H, Mangoni ML, Bhattacharjya S. NMR Structures and Interactions of Temporin-1Tl and Temporin-1Tb with Lipopolysaccharide Micelles MECHANISTIC INSIGHTS INTO OUTER MEMBRANE PERMEABILIZATION AND SYNERGISTIC ACTIVITY. *J Biol Chem*. 2011; 286(27):24394–406. <https://doi.org/10.1074/jbc.M110.189662> WOS:000292294900079. PMID: 21586570
 11. Sinha S, Zheng LZ, Mu YG, Ng WJ, Bhattacharjya S. Structure and Interactions of A Host Defense Antimicrobial Peptide Thanatin in Lipopolysaccharide Micelles Reveal Mechanism of Bacterial Cell Agglutination. *Sci Rep-Uk*. 2017; 7. ARTN 17795. <https://doi.org/10.1038/s41598-017-18102-6> WOS:000418359600045. PMID: 29259246
 12. Raetz CRH, Reynolds CM, Trent MS, Bishop RE. Lipid a modification systems in gram-negative bacteria. *Annu Rev Biochem*. 2007; 76:295–329. <https://doi.org/10.1146/annurev.biochem.76.010307.145803> WOS:000249336800014. PMID: 17362200
 13. Ernst RK, Hajjar AM, Tsai JH, Moskowitz SM, Wilson CB, Miller SI. Pseudomonas aeruginosa lipid A diversity and its recognition by Toll-like receptor 4. *J Endotoxin Res*. 2003; 9(6):395–400. <https://doi.org/10.1179/096805103225002764> WOS:000187716600009. PMID: 14733728
 14. Madala NE, Leone MR, Molinaro A, Dubery IA. Deciphering the structural and biological properties of the lipid A moiety of lipopolysaccharides from Burkholderia cepacia strain ASP B 2D, in Arabidopsis thaliana. *Glycobiology*. 2011; 21(2):184–94. <https://doi.org/10.1093/glycob/cwq146> WOS:000286717500006. PMID: 20943675
 15. Epand RF, Mowery BP, Lee SE, Stahl SS, Lehrer RI, Gellman SH, et al. Dual mechanism of bacterial lethality for a cationic sequence-random copolymer that mimics host-defense antimicrobial peptides. *J Mol Biol*. 2008; 379(1):38–50. <https://doi.org/10.1016/j.jmb.2008.03.047> WOS:000256642500005. PMID: 18440552
 16. Wiese A, Gutschmann T, Seydel U. Towards antibacterial strategies: studies on the mechanisms of interaction between antibacterial peptides and model membranes. *J Endotoxin Res*. 2003; 9(2):67–84. <https://doi.org/10.1179/096805103125001441> WOS:000183130800001. PMID: 12803879
 17. Nelson N, Schwartz DK. Single-Molecule Resolution of Antimicrobial Peptide Interactions with Supported Lipid A Bilayers. *Biophys J*. 2018; 114(11):2606–16. <https://doi.org/10.1016/j.bpj.2018.04.019> WOS:000434787900014. PMID: 29874611
 18. Hancock REW, Diamond G. The role of cationic antimicrobial peptides in innate host defences. *Trends Microbiol*. 2000; 8(9):402–10. [https://doi.org/10.1016/s0966-842x\(00\)01823-0](https://doi.org/10.1016/s0966-842x(00)01823-0) WOS:000089475800010. PMID: 10989307
 19. Oren Z, Lerman JC, Gudmundsson GH, Agerberth B, Shai Y. Structure and organization of the human antimicrobial peptide LL-37 in phospholipid membranes: relevance to the molecular basis for its non-cell-selective activity. *Biochem J*. 1999; 341:501–13. <https://doi.org/10.1042/0264-6021:3410501> WOS:000081871600005. PMID: 10417311
 20. Wang GS. Structures of Human Host Defense Cathelicidin LL-37 and Its Smallest Antimicrobial Peptide KR-12 in Lipid Micelles. *J Biol Chem*. 2008; 283(47):32637–43. <https://doi.org/10.1074/jbc.M805533200> WOS:000260893700053. PMID: 18818205
 21. Holak TA, Engstrom A, Kraulis PJ, Lindeberg G, Bennich H, Jones TA, et al. The Solution Conformation of the Antibacterial Peptide Cecropin-a—a Nuclear Magnetic-Resonance and Dynamical Simulated Annealing Study. *Biochemistry-U S*. 1988; 27(20):7620–9. <https://doi.org/10.1021/bi00420a008> WOS:A1988Q450100008. PMID: 3207693
 22. Wu JM, Jan PS, Yu HC, Haung HY, Fang HJ, Chang YI, et al. Structure and function of a custom anti-cancer peptide, CB1a. *Peptides*. 2009; 30(5):839–48. <https://doi.org/10.1016/j.peptides.2009.02.004> WOS:000266369900003. PMID: 19428759
 23. Ramirez LS, Pande J, Shekhtman A. Helical Structure of Recombinant Melittin. *J Phys Chem B*. 2019; 123(2):356–68. <https://doi.org/10.1021/acs.jpcc.8b08424> WOS:000456351000003. PMID: 30570258
 24. Kumagai A, Dupuy FG, Arsov Z, Elhady Y, Moody D, Ernst RK, et al. Elastic behavior of model membranes with antimicrobial peptides depends on lipid specificity and D-enantiomers. *Soft Matter*. 2019; 15(8):1860–8. <https://doi.org/10.1039/c8sm02180e> WOS:000459482400012. PMID: 30702120

25. Westphal O, Jann K. Bacterial Lipopolysaccharides Extraction with Phenol-Water and Further Applications of the Procedure. *Methods in Carbohydrate Chemistry*. 1965; 5:83–91.
26. Fischer W, Koch HU, Haas R. Improved Preparation of Lipoteichoic Acids. *Eur J Biochem*. 1983; 133(3):523–30. <https://doi.org/10.1111/j.1432-1033.1983.tb07495.x> WOS:A1983QY09900007. PMID: 6190649
27. Folch J, Lees M, Stanley GHS. A Simple Method for the Isolation and Purification of Total Lipides from Animal Tissues. *J Biol Chem*. 1957; 226(1):497–509. WOS:A1957WE89400051. PMID: 13428781
28. Hirschfeld M, Ma Y, Weis JH, Vogel SN, Weis JJ. Cutting edge: Repurification of lipopolysaccharide eliminates signaling through both human and murine toll-like receptor 2. *J Immunol*. 2000; 165(2):618–22. <https://doi.org/10.4049/jimmunol.165.2.618> WOS:000088085600002. PMID: 10878331
29. Caroff M, Tacken A, Szabo L. Detergent-Accelerated Hydrolysis of Bacterial-Endotoxins and Determination of the Anomeric Configuration of the Glycosyl Phosphate Present in the Isolated Lipid-a Fragment of the Bordetella-Pertussis Endotoxin. *Carbohydr Res*. 1988; 175(2):273–82. [https://doi.org/10.1016/0008-6215\(88\)84149-1](https://doi.org/10.1016/0008-6215(88)84149-1) WOS:A1988N153000010. PMID: 2900066
30. Neville F, Hodges CS, Liu C, Konovalov O, Gidalevitz D. In situ characterization of lipid A interaction with antimicrobial peptides using surface X-ray scattering. *Bba-Biomembranes*. 2006; 1758(2):232–40. <https://doi.org/10.1016/j.bbamem.2006.01.025> WOS:000237759200012. PMID: 16584708
31. Darwich Z, Klymchenko AS, Kucherak OA, Richert L, Mely Y. Detection of apoptosis through the lipid order of the outer plasma membrane leaflet. *Bba-Biomembranes*. 2012; 1818(12):3048–54. <https://doi.org/10.1016/j.bbamem.2012.07.017> WOS:000309801500016. PMID: 22846507
32. Baskin JM, Prescher JA, Laughlin ST, Agard NJ, Chang PV, Miller IA, et al. Copper-free click chemistry for dynamic in vivo imaging. *P Natl Acad Sci USA*. 2007; 104(43):16793–7. <https://doi.org/10.1073/pnas.0707090104> WOS:000250487600015. PMID: 17942682
33. Walder R, Nelson N, Schwartz DK. Super-resolution surface mapping using the trajectories of molecular probes. *Nat Commun*. 2011; 2. ARTN 515. <https://doi.org/10.1038/ncomms1530> WOS:000297686500002. PMID: 22044994
34. Walder R, Kastantin M, Schwartz DK. High throughput single molecule tracking for analysis of rare populations and events. *Analyst*. 2012; 137(13):2987–96. <https://doi.org/10.1039/c2an16219a> WOS:000304913100011. PMID: 22617120
35. Vila-Farres X, de la Maria CG, Lopez-Rojas R, Pachon J, Giralt E, Vila J. In vitro activity of several antimicrobial peptides against colistin-susceptible and colistin-resistant *Acinetobacter baumannii*. *Clin Microbiol Infec*. 2012; 18(4):383–7. <https://doi.org/10.1111/j.1469-0691.2011.03581.x> WOS:000301646100019. PMID: 21672084
36. Rangel K, Lechuga GC, Souza ALA, da Silva Carvalho JPP, Villas Bôas MHS, De Simone SG. Pan-Drug Resistant *Acinetobacter baumannii*, but Not Other Strains, Are Resistant to the Bee Venom Peptide Melittin. *Antibiotics*. 2020; 9:178.
37. Feng XR, Sambanthamoorthy K, Palys T, Paranaivitana C. The human antimicrobial peptide LL-37 and its fragments possess both antimicrobial and antibiofilm activities against multidrug-resistant *Acinetobacter baumannii*. *Peptides*. 2013; 49:131–7. <https://doi.org/10.1016/j.peptides.2013.09.007> WOS:000326941100018. PMID: 24071034
38. Jaskiewicz M, Neubauer D, Kazor K, Bartoszewska S, Kamysz W. Antimicrobial Activity of Selected Antimicrobial Peptides Against Planktonic Culture and Biofilm of *Acinetobacter baumannii*. *Probiotics Antimicro*. 2019; 11(1):317–24. <https://doi.org/10.1007/s12602-018-9444-5> WOS:000471045000034. PMID: 30043322
39. Xia LJ, Liu ZY, Ma J, Sun SR, Yang JH, Zhang FC. Expression, purification and characterization of cecropin antibacterial peptide from *Bombyx mori* in *Saccharomyces cerevisiae*. *Protein Express Purif*. 2013; 90(1):47–54. <https://doi.org/10.1016/j.pep.2013.02.013> WOS:000320293500007. PMID: 23500722
40. Dosler S, Karaaslan E, Gerceker AA. Antibacterial and anti-biofilm activities of melittin and colistin, alone and in combination with antibiotics against Gram-negative bacteria. *J Chemotherapy*. 2016; 28(2):95–103. <https://doi.org/10.1179/1973947815y.0000000004> WOS:000377444700004. PMID: 25801062
41. Pandey BK, Ahmad A, Asthana N, Azmi S, Srivastava RM, Srivastava S, et al. Cell-Selective Lysis by Novel Analogues of Melittin against Human Red Blood Cells and *Escherichia coli*. *Biochemistry-US*. 2010; 49(36):7920–9. <https://doi.org/10.1021/bi100729m> WOS:000281471600018. PMID: 20695504
42. Turner J, Cho Y, Dinh NN, Waring AJ, Lehrer RI. Activities of LL-37, a cathelin-associated antimicrobial peptide of human neutrophils. *Antimicrob Agents Ch*. 1998; 42(9):2206–14. <https://doi.org/10.1128/AAC.42.9.2206> WOS:000075737400010. PMID: 9736536
43. Luo Y, McLean DTF, Linden GJ, McAuley DF, McMullan R, Lundy FT. The Naturally Occurring Host Defense Peptide, LL-37, and Its Truncated Mimetics KE-18 and KR-12 Have Selected Biocidal and

- Antibiofilm Activities Against *Candida albicans*, *Staphylococcus aureus*, and *Escherichia coli* In vitro. *Front Microbiol.* 2017; 8. ARTN 544 <https://doi.org/10.3389/fmicb.2017.00544> WOS:000397977800001. PMID: 28408902
44. Gunasekera S, Muhammad T, Stromstedt AA, Rosengren KJ, Goransson U. Backbone Cyclization and Dimerization of LL-37-Derived Peptides Enhance Antimicrobial Activity and Proteolytic Stability. *Front Microbiol.* 2020; 11. ARTN 168. <https://doi.org/10.3389/fmicb.2020.00168> WOS:000524523200001. PMID: 32153522
 45. Romoli O, Mukherjee S, Mohid SA, Dutta A, Montali A, Franzolin E, et al. Enhanced Silkworm Cecropin B Antimicrobial Activity against *Pseudomonas aeruginosa* from Single Amino Acid Variation. *Acs Infect Dis.* 2019; 5(7):1200–13. <https://doi.org/10.1021/acinfecdis.9b00042> WOS:000475825800016. PMID: 31045339
 46. Wang JR, Ma K, Ruan MS, Wang YJ, Li Y, Fu YV, et al. A novel cecropin B-derived peptide with anti-bacterial and potential anti-inflammatory properties. *Peerj.* 2018; 6. ARTN e5369 <https://doi.org/10.7717/peerj.5369> WOS:000439944000011. PMID: 30065898